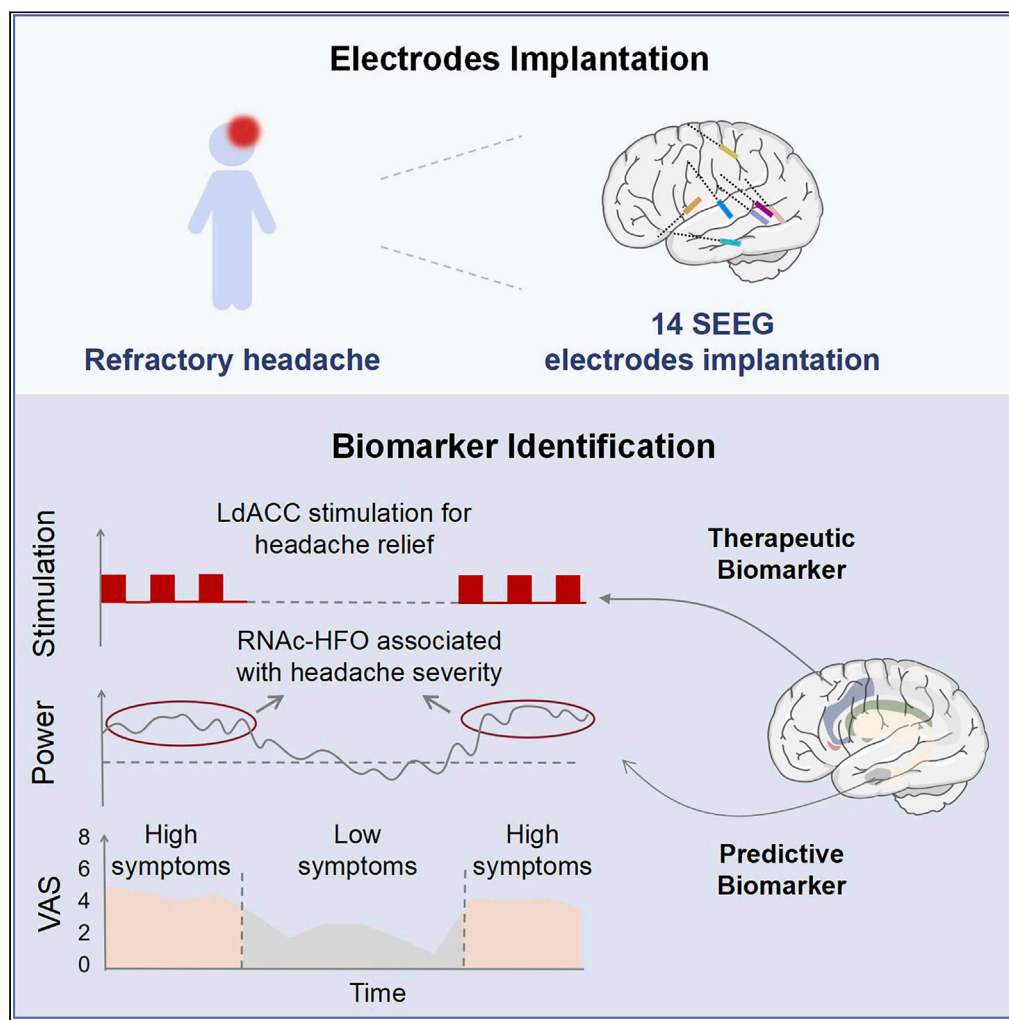**Article**

A pilot study on a patient with refractory headache: Personalized deep brain stimulation through stereoelectroencephalography

Hulin Zhao,
Shuhua Zhang,
Yining Wang, ...,
Chien-Hung Yeh,
Zhao Dong,
Shengyuan Yu

chien-hung.yeh@bit.edu.cn
(C.-H.Y.)
dong_zhaozhao@126.com
(Z.D.)

Highlights

RNAc-HFO may serve as a valuable biomarker for characterizing the headache severity

LdACC may serve as a precise DBS target for refractory chronic migraine

Personalized DBS circuit positioning is a prominent trend in precision therapy

Article

A pilot study on a patient with refractory headache: Personalized deep brain stimulation through stereoelectroencephalography

Hulin Zhao,[1,7] Shuhua Zhang,[2,3,7] Yining Wang,[4,7] Chuting Zhang,[4] Zihua Gong,[2,3] Mingjie Zhang,[2,3] Wei Dai,[2,3] Ye Ran,[2,3] Wenbin Shi,[4,5] Yuanyuan Dang,[1] Aijun Liu,[1] Zhengbo Zhang,[6] Chien-Hung Yeh,[4,5,8,*] Zhao Dong,[2,3,8,9,*] and Shengyuan Yu[2,3]

SUMMARY

The integration of stereoelectroencephalography with therapeutic deep brain stimulation (DBS) holds immense promise as a viable approach for precise treatment of refractory disorders, yet it has not been explored in the domain of headache or pain management. Here, we implanted 14 electrodes in a patient with refractory migraine and integrated clinical assessment and electrophysiological data to investigate personalized targets for refractory headache treatment. Using statistical analyses and cross-validated machine-learning models, we identified high-frequency oscillations in the right nucleus accumbens as a critical headache-related biomarker. Through a systematic bipolar stimulation approach and blinded sham-controlled survey, combined with real-time electrophysiological data, we successfully identified the left dorsal anterior cingulate cortex as the optimal target for the best potential treatment. In this pilot study, the concept of the herein-proposed data-driven approach to optimizing precise and personalized treatment strategies for DBS may create a new frontier in the field of refractory headache and even pain disorders.

INTRODUCTION

Migraine is a common neurovascular disorder and the second leading cause of disability worldwide according to the 2016 Global Burden of Disease.[1,2] Chronic migraine, defined as a headache occurring on ≥ 15 days per month for >3 months with migraine occurring on ≥ 8 of these days,[3] is associated with even greater disability, indicating the need for effective treatment. The current conventional treatments include both pharmacological and non-pharmacological therapies, but approximately 3%–5.1% of patients with refractory chronic migraine (rCM) showed minimal or no response to standard and/or active treatment.[1,4] For this minute portion of patients, non-invasive neuromodulation techniques such as transcutaneous electrical stimulation and transcranial magnetic stimulation, combined with the administration of multiple medications, have proven to be ineffective.[5] As a result, it is imperative to explore new therapeutic alternatives, such as deep brain stimulation (DBS).

As a well-established therapy, DBS has been used for treatment-resistant conditions such as movement disorders, psychiatric disorders, epilepsy, and pain syndromes (e.g., neuropathic pain and cluster headache).[6] Some studies have successfully demonstrated the analgesic effects and functional improvement achieved through DBS in patients with chronic pain[7] or depression.[8] Furthermore, the administration of DBS has been observed to alleviate or exacerbate migraine symptoms in certain patients, indicating the potential of DBS as a treatment option for migraines.[9–11] A recent meta-analysis showed that DBS for treatment of refractory chronic cluster headache (rCCH) had a pooled response rate of only 77%, with high heterogeneity of results.[12] Moreover, the only randomized placebo-controlled double-blind trial of DBS in patients with rCCH to date did not support the efficacy of this treatment.[13] Previous studies have shown that the variable efficacy of DBS for rCCH may be due not only to misalignment of electrodes but also to the non-individualized stimulation target, the complicated pathophysiological or disease state, and the individual structure or functional anatomy of the patient.[12,14] In addition to these issues, the multi-oscillatory neural dynamics and the heterogeneity of neural circuits in the brain have made optimizing and allocating individualized stimulation regimens for precise treatment of headaches by DBS a major challenge. Some recent studies of DBS for patients with treatment-resistant depression have explored individualized targets with stereoelectroencephalography (SEEG) electrodes,[8,15] providing encouraging findings regarding

[1]Department of Neurosurgery, The First Medical Center, Chinese PLA General Hospital, Beijing 100853, China
[2]Department of Neurology, Chinese PLA General Hospital, Beijing 100853, China
[3]International Headache Centre, Chinese PLA General Hospital, Beijing 100853, China
[4]School of Information and Electronics, Beijing Institute of Technology, Beijing 100081, China
[5]Key Laboratory of Brain Health Intelligent Evaluation and Intervention, Beijing Institute of Technology, Ministry of Education, Beijing 100081, China
[6]Center for Artificial Intelligence in Medicine, Chinese PLA General Hospital, Beijing 100853, China
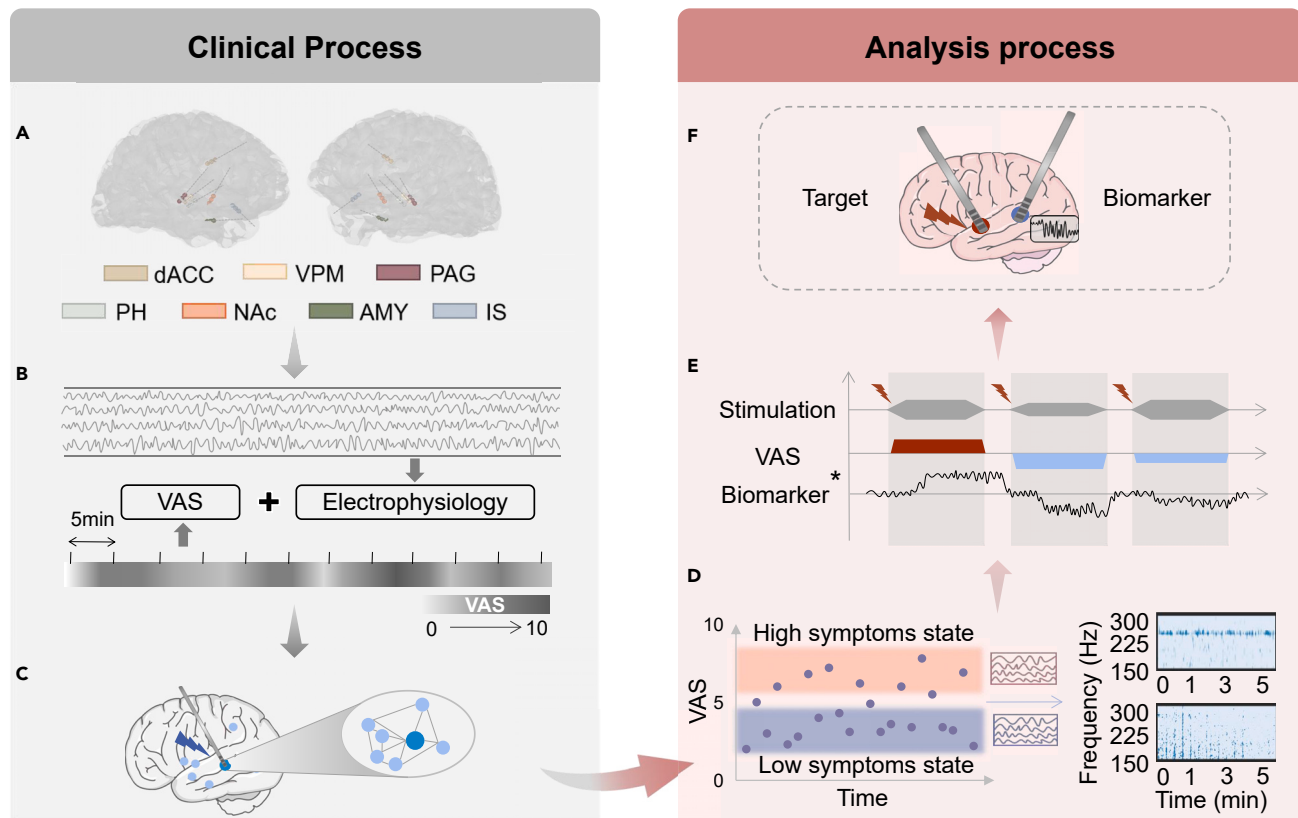[7]These authors contributed equally
[8]These authors contributed equally
[9]Lead contact
*Correspondence: chien-hung.yeh@bit.edu.cn (C.-H.Y.), dong_zhaozhao@126.com (Z.D.)
https://doi.org/10.1016/j.isci.2024.108847

Figure 1. Study procedure

(A) Implantation and visualization of the 14 SEEG electrodes.

(B) Clinical monitoring and electrophysiological recordings. Headache severity was recorded in 5-min increments using a visual analog scale (VAS) and real-time electrophysiological recordings (SEEG). The VAS was used to rate the intensity of the headache and ranged from 0 to 10, with 0 representing no pain and 10 representing the most severe pain.

(C) Stimulation parameters were varied across the contacts in all brain regions to assess the clinical effects and validate the clinical-electrophysiological analyses. This approach enabled the identification of changes in functional connectivity among brain regions, with the stimulated brain region represented by dark blue, and the brain regions exhibiting significant changes in response to headache intensity represented by light blue. The SEEG data, VAS scores, and other responses (e.g., physiological responses induced by the stimulation or headache-related concomitant symptoms) were all recorded simultaneously in real time during stimulation.

(D) Clinical and electrophysiological features from the monitoring period were combined to determine the biomarker responding to the headache fluctuation. According to the VAS assessment and SEEG data, the intensity of headache was divided into two states (pink: high-symptom state; blue: low-symptom state), and biomarkers determined by real-time SEEG analyses reflected the various headache states.

(E) Clinical and electrophysiological data from the monitoring period were combined to determine the best stimulating target for maximum headache relief. For the stimulus data, fluctuations in headache intensity during stimulation (exacerbation, no change, or improvement) were matched with corresponding changes in the biomarker to determine the best target, supported by both the clinical response and electrophysiology. Red indicates a worsening headache, whereas blue indicates the opposite. The line width in the stimulation denotes the stimulus intensity. *Biomarker refers to the spectral power feature that optimally reflects varying headache states.

(F) The optimization of both the stimulation targets and biomarkers served to initiate biomarker-directed personalized stimulation of DBS. SEEG, stereoelectroencephalography; VAS, visual analog scale; PAG/PVG, periaqueductal/periventricular gray area; VPM/VPL, ventral posteromedial/ventral posterolateral; NAc, nucleus accumbens; dACC, dorsal anterior cingulate cortex; PH, posterior hypothalamus; AMY, amygdala; IS, insula.

precise treatment of refractory headaches with DBS. To the best of our knowledge, however, no case reports have described the precise treatment of refractory headaches or even pain by integrating clinical assessment and electrophysiological data. Therefore, we hypothesized that SEEG recordings can be used to access headache intensity-linked biomarkers that will aid in brain region identification, identifying specific targets for the first application of DBS for rCM to date.

RESULTS

Clinical characteristics and procedure for electrode implantation

The patient was a young man with more than 5-year history of chronic migraine, unresponsive to multiple preventive treatments (antidepressants, antiepileptics, beta-blockers, calcium channel blockers, onabotulinumtoxin A, etc.) and non-pharmacological treatments.
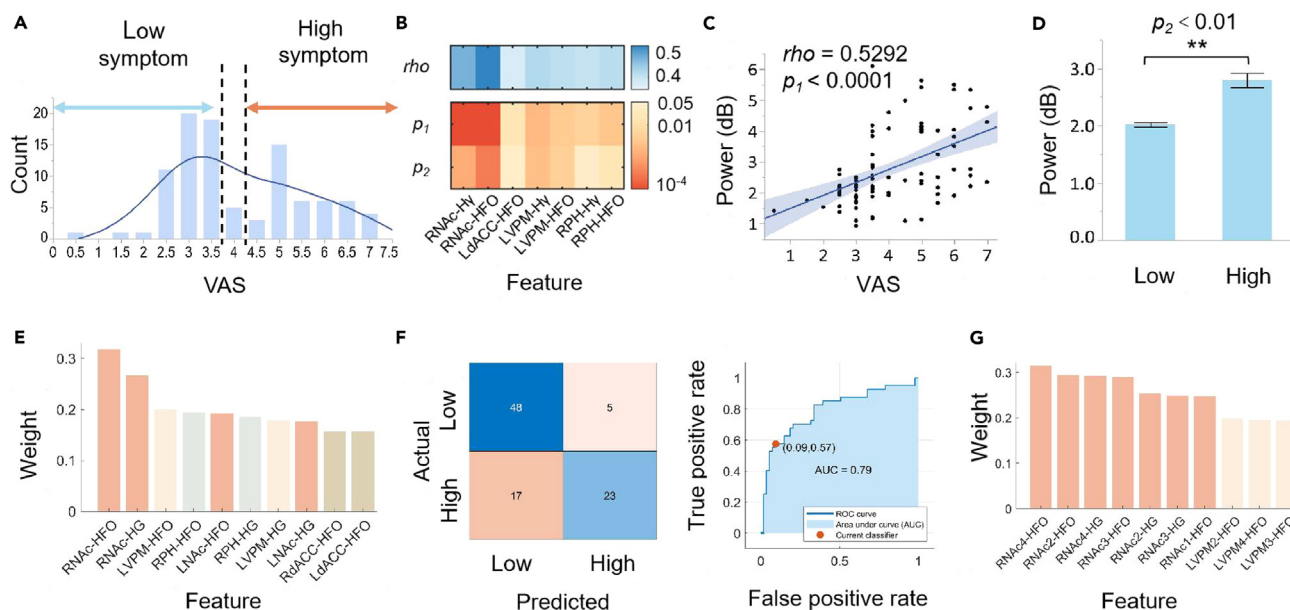
Figure 2. Identification of pain-related biomarkers

(A) VAS scores distribution during the monitoring ranged from 0.5 to 7.5. After the elimination of the "moderate" symptom group (VAS = 4), the dataset was re-categorized into a "low" symptoms group (VAS of 0.5–3.5) and a "high" symptoms group (VAS of 4.5–7.5).

(B) The relationship and discrimination of spectral power features and VAS scores. RNAc-HFO had the most striking features among the seven power characteristics that were significantly associated with and distinct from the VAS. rho, p_1: Spearman's correlation coefficient along with its p value between power and VAS scores; p_2: Wilcoxon rank-sum test result representing the difference in power between the low and high migraine symptom groups.

(C) Correlation of RNAc-HFO band power and VAS scores. Each point represents a VAS score and the corresponding RNAc-HFO band power for a specific trial (total of 98 data points).

(D) The ability of the RNAc-HFO band power to discriminate between high- and low-symptom groups. Bar heights indicate mean values, and black error bars indicate the standard errors. *p < 0.05, **p < 0.01, ***p < 0.001.

(E) Ranking of all extracted features using the F-score feature selection algorithm, with the highest weight indicating the greatest ability to discriminate between the high- and low-symptom groups. The greatest headache discriminatory ability was demonstrated by RNAc-HFO. HG: high gamma.

(F) Cross-validated machine-learning models. Features with weights >0.25 and p1 and p2 < 0.05 were chosen as input to the classifier (the HFO band power in the RNAc), with the confusion matrix and ROC curve representing the performance of the optimal classifier (SVM).

(G) Ranking of contact features using the F-score feature selection algorithm, and the HFO of the various contacts of the RNAC all had higher weights.

Following a thorough evaluation and observation, the patient underwent SEEG in preparation for precise DBS treatment. The patient's medication regimen during the SEEG recordings remained consistent with that of the preoperative period and has been maintained for over 6 months, ensuring relative stability of the individual brain network for this patient (Table S2). The patient was implanted with 14 SEEG electrodes for clinical and electrophysiological process, to investigate a personalized target for treatment. During the clinical process, clinical assessment and electrophysiological data were obtained through monitoring and stimulation. During the analysis process, statistical analyses and cross-validated machine-learning models were used for identification of biomarker and stimulation targets (Figure 1). The patient reported complete pain relief after implantation of the SEEG electrodes, in contrast to the preoperative visual analogue scale (VAS) scores of 4–7. When the clinical-electrophysiological recording was started, the patient used typical triggers according to the headache diary to provoke migraine attacks, with VAS scores of 0.5–7.5, which exhibited clinical features similar to those of past spontaneous migraine attacks. Following the clinical monitoring and mapping, the patient gradually experienced more spontaneous migraine attacks while waiting for the DBS procedure, as he had previously, but with a VAS score of only 1 to 2. The preoperative dosage regimen was followed throughout the study and was still in use at the time of writing. During the 6-month postoperative follow-up, the patient's headache attacks worsened in severity and frequency, becoming comparable to the preoperative headaches. However, due to personal preference and the availability of calcitonin gene-related peptide (CGRP) currently, the patient chose to temporarily delay DBS implantation.

High-frequency oscillation (HFO) in the right nucleus accumbens (RNAc) as a crucial pain-related biomarker linked to pain fluctuations

According to the distribution of the VAS dataset, we eliminated the "moderate" symptoms group (VAS = 4) and reclassified the data into a "low" symptoms group (VAS of 0.5–3.5) and a "high" symptoms group (VAS of 4.5–7.5) (Figure 2A). Seven power characteristics were

Table 1. Significant power characteristics statistics in different brain regions

	RNAc-HFO[a]	RNAc-Hγ[a]	LNAc-Hγ[a]	LNAc-HFO[a]	LdACC-HFO[a]	LVPM-Hγ[a]	LVPM-HFO[a]
rho[a]	0.5292	0.4786	0.3701	0.3816	0.3721	0.4198	0.4070
p_1[a]	<0.0001	<0.0001	<0.0001	<0.0001	0.0181	0.0019	0.0036
p_2[a]	0.0003	0.0012	0.0457	0.0372	0.0408	0.0024	0.0044

[a]rho, p_1, Spearman correlation, representing correlation between power and VAS scores; p_2, Wilcoxon rank-sum test, representing variability of power between low and high migraine symptoms; Hγ, High gamma; HFO, High-frequency oscillation.

significantly correlated with and differed from the VAS score (Table 1), with HFO in the RNAc (RNAc-HFO) being the most strongly correlated with the VAS score (rho = 0.5292, p < 0.0001) (Figures 2B and 2C) and significantly differing between the mild and severe pain levels (p = 0.0003) (Figure 2D). The characteristic ranking also revealed the greatest weighting of HFO in the RNAc brain region (Figure 2E). Features with corresponding weights of >0.25 and both p1 and p2 values of <0.05 demonstrated that the linear support vector machine (SVM) out-performed the other classifiers. Compared with other biomarkers, RNAc-HFO had the optimal performance with an accuracy and area under the receiver operating curve (AUC) of 76.34% and 0.79, respectively (Figures 2F; Table 2; Tables S3 and S4). On the other side, power features from all brain regions were used as inputs to the machine-learning models. The results revealed that the linear SVM model was still optimal, with an accuracy of 71.43%; however, this accuracy was lower than that of the model using only the HFO-band power from the RNAc (Table 3). The correlation, significance analyses, and characteristic ranking of all contacts in the regions of interest supported the optimal discrimination of HFOs on the four contacts of the RNAc (Figures 2G; Table 4).

Left dorsal anterior cingulate cortex (LdACC) as an optimal target for personalized DBS

Different stimulus parameters elicited varying responses in different regions, including pain responses and other associated symptoms; these included typical accompanying symptoms, autonomic symptoms, and olfactory hallucination, all of which were associated with the patient's previous migraine attacks. Clinically, the patient reported a reduction in headache severity during stimulation in two brain regions (LdACC and RNAc), with varying degrees of headache exacerbation in most other brain regions (Figure 3A). Based on the VAS scores reported during the 5-day stimulation period, we identified the LdACC as the most effective stimulation target (Figure 3B). Pre- and post-stimulus VAS scores showed significantly greater improvement (p = 0.006) when compared with the RNAc (p = 0.081) (Figure 3C). In terms of electrophysiology, the power of RNAc-HFO exhibited a consistent decrease following stimulation in trials resulting in headache relief (Figure 3D). Conversely, the opposite trend was observed in trials resulting in headache exacerbation (Figure S1A), while no significant alteration in power was noted in trials where headache severity remained unchanged (Figure S1B). This validation confirms the efficacy of RNAc-HFO as a biomarker for assessing pain severity. Among these effects, the stimulation of LdACC produced a significant difference in electrophysiological effects (p < 0.01) (Figure 3E). Furthermore, the low-frequency phase of the LdACC had a significant modulatory effect on the HFO band amplitude of the RNAc, which was increased in the high-symptom state. This confirmed the modulatory effect of the LdACC on the RNAc during headache fluctuation (Figure 3F).

DISCUSSION

In this study, we developed a personalized strategy through multidimensional and multi-perspective analysis. First, we tracked the baseline period of the patient's headache attacks using VAS scores and electrophysiology, to characterize the various headache states. Based on the clinical state of "low" or "high" symptoms, the corresponding electrophysiology data were combined to identify the biomarker that characterized the optimal state for this patient, which was originally explored in previous migraine and EEG studies.[16,17] On the one hand, biomarker research facilitates the identification of personalized key targets against the complexity of individual brain networks due to pathophysiology. On the other hand, the current trend in DBS implementation is the initiation of biomarker-based on-demand stimulation via biomarker monitoring.[6] Second, in terms of therapeutic targeting, we first intuitively identified the best stimulus target for patient comfort using personalized stimulus-response mapping. When improvement was noted in the subjective headache symptom ratings, which is an important indicator of efficacy, we could identify the target of stimulation to some extent. However, because subjective feelings have certain confounding factors, such as emotions and perceptions, we further validated this with objective data drivers. In conjunction with the biomarker identified in the first step, we paired the monitoring state signal with clinical symptoms and successfully validated the relationship between a decline in the biomarker and headache improvement, to objectively determine the physiological effect of the stimulus target. In addition, phase-amplitude coupling in this study was used to validate the functional modulation between the biomarker and stimulated regions, confirming that the modulation between the two is an important link in clinical effects. Although the final stimulation efficacy is subject to further investigation, the multidimensionally validated trial protocol ensures the best possible treatment.

In the present study, RNAc-HFO optimally reflected pain fluctuations with a positive association. Previous research has suggested that the nucleus accumbens (NAc) could be used as a biomarker for pain or migraine, with a decrease in the volume of the RNAc as shown through neuroimaging studies[18] and increased functional connectivity in the RNAc with some brain regions in patients with migraine.[19] Iron deposition

Table 2. Comparisons of the performances of different classifiers using features of all brain regions of RNAc-HFO

Classifier	Acc.	Spec.	Sen.	F1- score	AUC
DT[a]	67.74%	73.58%	60.00%	61.54%	0.71
LDA[a]	73.12%	75.47%	70.00%	69.14%	0.78
LR[a]	76.34%	90.57%	57.50%	67.65%	0.78
NB[a]	75.27%	90.57%	55.00%	65.67%	0.77
SVM[a]	76.34%	90.57%	57.50%	67.65%	0.79

[a]Features with weights greater than 0.25, and both p_1 and p_2 values less than 0.05 were selected as input to the classifiers (the HFO band power in the RNAc). Linear SVM outperformed other classifiers when using only the HFO band power of the RNAc for classification, with accuracy, specificity, sensitivity, F1-score, and AUC remaining at 76.34%, 90.57%, 57.50%, 67.65%, and 0.79, respectivel. DT, Decision Trees; LDA, Linear Discriminant Analysis; LR, Logistic Regression; NB, Naive Bayes; SVM, Support Vector Machines.

in the NAc may be a biomarker for migraine chronicity and migraine-related dysfunctions.[20] Furthermore, we identified the most prominent biomarkers, RNAc-4 and RNAc-2, which are localized within the shell of NAc. Notably, extensive prior research has demonstrated that the shell of NAc plays a pivotal role in limbic system functions such as reward and pain processing. This region receives glutamatergic projections from the limbic system, including the anterior cingulate cortex (ACC), as well as dopaminergic projections from the ventral tegmental area (VTA),[21] while also exhibiting efferents to the diencephalon and pallidal complex.[22] Importantly, the presence of dynorphin-containing neurons and kappa opioid receptor (KOR) activity within the NAc shell are both essential and sufficient to induce negative affective states associated with pain.[23] Supporting this notion, De Felice et al. observed an increase in dopamine release from the NAc shell in an animal model of "headache" through direct stimulation of dural injury receptors, which could be effectively suppressed by prior systemic administration of sumatriptan.[24] However, further mechanistic investigation is still warranted to fully elucidate the precise role of the NAc in the pathogenesis of migraines.

Furthermore, we identified the LdACC as the most effective target region for the patient based on his clinical response and further validation of biomarkers that could be improved, which is an important step in personalized treatment. Some studies have shown that functional changes in the ACC might serve as a biomarker for migraine prevention. Changes in cortical thickness in the left posterior cingulate,[25] increases in gamma-aminobutyric acid levels in the ACC or posterior cingulate,[26,27] and the blood oxygenation level-dependent response in the perigenual region of the right ACC[28] have all been linked to clinical aspects of migraine such as headache frequency and intensity. These findings support our hypothesis that the ACC might be used as a potential therapeutic target for migraine. Furthermore, the modulatory effects of electrical stimulation in the ACC and RNAc-HFO on migraine in our study demonstrated that functional regulation between the ACC and NAc may be involved in migraine pathophysiology. Optogenetics have revealed that the ACC projection to the NAc pathway is selectively involved in pain and analgesia social transfer, implying that the NAc is a downstream target of ACC pain modulation.[29] The ACC most likely mediates pain-related aversive behavior by projecting to NAc D2-type medium spiny neurons and other mesolimbic dopamine systems.[30] Thus, we hypothesize that a similar pathway exists in migraine, which supports the feasibility of the LdACC as a therapeutic target in our study. However, specific molecular mechanisms should be investigated further. More importantly, the effectiveness must be validated based on the patient's follow-up outcome after DBS placement.

Interestingly, the patient reported an approximately 2-week absence of migraine attack after SEEG implantation; the migraine attacks then gradually returned during the subsequent follow-up. Given the results of previous studies on SEEG or DBS implantation, we speculate that several factors may be at work in this phenomenon. First, Hamani et al. reported that patients with chronic neuropathic pain may suffer a substantial reduction in pain scores in the absence of stimulation, referred to as the "insertional effect."[31,32] Remarkably, this pre-stimulation analgesic effect served as a significant predictor of favorable postoperative outcomes.[31,32] And it has been shown that the absence of insertional effect could aid in the indirect assessment of whether the electrodes are in the proper target position.[33] Thus, the insertional effect at the LdACC may have temporarily relieved the patient's migraine, corroborating the validity of the subsequent stimulation mapping. Second, some research has suggested that subanesthetic doses of propofol could be used in the acute or prophylactic treatment of intractable migraine, with efficacy lasting up to 6 months[34,35]; however, this needs to be confirmed. The intraoperative maintenance of anesthesia in our patient had the potential to result in headache relief followed by recurrence of migraine 2 weeks later. However, the validity of this conjecture is difficult to confirm based on the available information. Furthermore, the placebo effect is important in both DBS[36,37] and SEEG implantation. In fact, some studies have shown that more invasive procedures have a larger placebo effect[38]; thus, we cannot completely rule out the possibility of a placebo effect causing bias in the patient's assessment of symptoms. However, the placebo-controlled blind stimulation procedures as well as the double-blind stimulation recording and data analyses in our study are expected to have reduced the placebo effect in our patient.

This is the first study to evaluate SEEG recordings in a patient with migraine, to deliver precise and personalized DBS. To provide specialized care, we identified the LdACC as a therapeutic target for DBS using the biomarker of HFO in the RNAc. To determine the efficacy of this treatment approach, we plan to perform DBS implantation and monitor this patient for a long time. Our preliminary study conclusively shows that this unique concept for tailored DBS in patients with rCM is feasible, and we anticipate further verification of its precise therapeutic use in various forms of headaches and even pain.

Table 3. Comparisons of the performances of different classifiers using features of different contacts in brain regions

Classifier	Acc.	Spec.	Sen.	F1- score	AUC
DT[a]	63.39%	75.47%	62.22%	65.12%	0.68
LDA[a]	67.35%	64.15%	71.11%	66.67%	0.68
LR[a]	56.12%	50.94%	62.22%	56.57%	0.58
NB[a]	59.18%	50.94%	68.89%	60.78%	0.77
SVM[a]	71.43%	77.36%	64.44%	67.44%	0.76

[a]Features of different contacts in brain regions were selected as input to the classifiers, and linear SVM outperformed other classifiers with accuracy, specificity, sensitivity, F1-score, and AUC remaining at 71.43%, 77.36%, 64.44%, 67.44%, and 0.76, respectively. DT, Decision Trees; LDA, Linear Discriminant Analysis; LR, Logistic Regression; NB, Naive Bayes; SVM, Support Vector Machines.

Limitations of the study

This is the first study to explore personalized targets for DBS treatment of rCM to date. However, it has several limitations. First, because this was an individualized design for one patient, the results cannot be generalized to other patients with migraine. Second, the calibration of the clinical recording and stimulation responses may be influenced by certain subjective factors, such as emotions; therefore, we trained the patient in advance for recording and increased the number of trials to ensure accuracy. Third, we employed varied stimulation durations and washout periods in our experimental design to examine the patient's headache recordings, with the objective of identifying precise targets based on the observed acute effects of brain region stimulation. Nonetheless, it remains a possibility that certain brain regions with initial non-effect could potentially exhibit therapeutic benefits through prolonged stimulation. Consequently, this alternative perspective warrants further investigation as a viable research avenue. Meanwhile, although a 60-s washout period has been set, it is still not fully guaranteed that bleed-over effects or cumulative effects between trials did not occur. Furthermore, some therapeutic regimens, such as CGRP antagonists and monoclonal antibodies to CGRP or its receptor, were not available in China before the study and could not be administered to our patient; as a result, their efficacy remains unknown. Finally, because the patient was highly satisfied with his clinical condition at the time of SEEG electrode removal, the second step of DBS implantation was postponed and will be scheduled later based on his condition and personal preferences.

STAR★METHODS

Detailed methods are provided in the online version of this paper and include the following:

- KEY RESOURCES TABLE
- RESOURCE AVAILABILITY
  - Lead contact
  - Materials availability
  - Data and code availability
- EXPERIMENTAL MODEL AND STUDY PARTICIPANT DETAILS
  - Participant
  - Standard protocol approvals, registrations, and patient consents
- METHOD DETAILS

Table 4. Significant power characteristics statistics in different contacts in brain regions

	RNAc-1 HFO[a]	RNAc-2 Hγ[a]	RNAc-2 HFO[a]	RNAc-3 Hγ[a]	RNAc-3 HFO[a]	RNAc-4 Hγ[a]	RNAc-4 HFO[a]
rho	0.4511	0.4947	0.5367	0.4953	0.5300	0.5289	0.5449
p_1	0.0011	0.0001	<0.0001	<0.0001	<0.0001	<0.0001	<0.0001
p_2	0.0145	0.0033	0.0008	0.0041	0.0015	0.0004	0.0005
	LVPM-1 Hγ[a]	LVPM-2 Hγ[a]	LVPM-2 HFO[a]	LVPM-3 Hγ[a]	LVPM-3 HFO[a]	LVPM-4 Hγ[a]	LVPM-4 HFO[a]
rho	0.4143	0.4002	0.3954	0.4149	0.4108	0.4294	0.4334
p_1	0.0010	0.0199	0.0250	0.0097	0.0119	0.0046	0.0037
p_2	0.0276	0.0164	0.0223	0.0113	0.0164	0.0044	0.0085

[a]Hγ, High gamma; HFO, High-frequency oscillation.
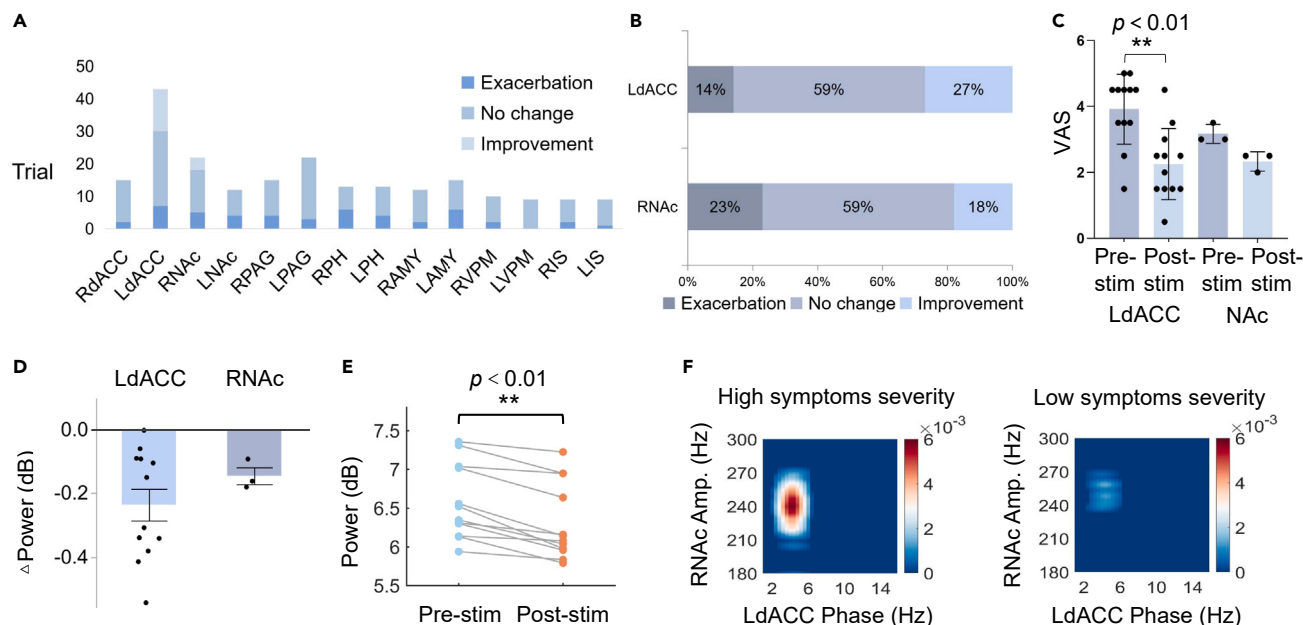
Figure 3. Identification of the optimal stimulation target

(A) Pain responses to various stimuli in various regions. Aggravation is represented by deep blue, while relief is represented by light blue. Following stimulation, only two brain regions, RNAc and LdACC, exhibited improvement in headache intensity.

(B) Stimulation responses of the two optional regions, i.e., improvement, unchanged, or exacerbation.

(C) Distribution of VAS scores pre- and post-stimulation in LdACC and RNAc, with a statistically significant difference in the former. **p < 0.01.

(D) Validation of the biomarker against the data showed a decrease in post-stimulation power in trials with improvement in headache severity, more pronounced in LdACC.

(E) Statistical analysis of RNAc-HFO power variation pre- and post-stimulation in LdACC before and after stimulation on data with headache improvement. In data where stimulation caused headache improvement, there was a decrease in the corresponding biomarker power. **p < 0.01.

(F) Verification of functional modulation between RNAc and LdACC using phase-amplitude coupling (PAC). The low-frequency phase of LdACC had a great modulatory effect on the HFO band amplitude of RNAc, which was enhanced in the high-symptom state.

- ○ Surgical procedure
- ○ Clinical measures of migraine and associated comorbidities
- ○ Clinical-electrophysiological mapping via electrode stimulation
- ○ Signal processing
- ○ Biomarker discovery for headache states representation
- ● QUANTIFICATION AND STATISTICAL ANALYSIS

AUTHOR CONTRIBUTIONS

Conceptualization, H.Z., C.-H.Y., Z.D., and S.Y.; methodology, H.Z., S.Z., Y.W., and C.Z.; validation, S.Z. and Y.W.; formal analysis, Y.W., C.Z., W.S., and C.Z.; investigation, H.Z., S.Z., Z.G., and Z.Z.; resources, M.Z., Y.D., and A.L.; data curation, S.Z. and Y.W.; writing – original draft, S.Z. and Y.W.; writing – review & editing, H.Z., C.-H.Y., and Z.D.; visualization, W.D. and Y.R.; supervision, C.-H.Y. and Z.D.; funding acquisition, C.-H.Y. and Z.D.

DECLARATION OF INTERESTS

The authors declare no competing interests.

REFERENCES

1. Parreira, E., Luzeiro, I., and Pereira Monteiro, J.M. (2020). [Chronic and Refractory Migraine: How to Diagnose and Treat]. Acta Med. Port. *33*, 753–760.

2. GBD 2016 Disease and Injury Incidence and Prevalence Collaborators (2017). Global, regional, and national incidence, prevalence, and national incidence, prevalence, and years lived with disability for 328 diseases and injuries for 195 countries, 1990-2016: a systematic analysis for the Global Burden of Disease Study 2016. Lancet *390*, 1211–1259.

3. (2018). Headache Classification Committee of the International Headache Society (IHS) the International Classification of Headache Disorders, 3rd edition. Cephalalgia *38*, 1–211.

4. Irimia, P., Palma, J.A., Fernandez-Torron, R., and Martinez-Vila, E. (2011). Refractory migraine in a headache clinic population. BMC Neurol. *11*, 94.

5. Knotkova, H., Hamani, C., Sivanesan, E., Le Beuffe, M.F.E., Moon, J.Y., Cohen, S.P., and Huntoon, M.A. (2021). Neuromodulation for chronic pain. Lancet (London, England) *397*, 2111–2124.

6. Krauss, J.K., Lipsman, N., Aziz, T., Boutet, A., Brown, P., Chang, J.W., Davidson, B., Grill, W.M., Hariz, M.I., Horn, A., et al. (2021). Technology of deep brain stimulation: current status and future directions. Nat. Rev. Neurol. *17*, 75–87.

7. Shirvalkar, P., Prosky, J., Chin, G., Ahmadipour, P., Sani, O.G., Desai, M., Schmitgen, A., Dawes, H., Shanechi, M.M., Starr, P.A., and Chang, E.F. (2023). First-in-human prediction of chronic pain state using intracranial neural biomarkers. Nat. Neurosci. *26*, 1090–1099.

8. Scangos, K.W., Khambhati, A.N., Daly, P.M., Makhoul, G.S., Sugrue, L.P., Zamanian, H., Liu, T.X., Rao, V.R., Sellers, K.K., Dawes, H.E., et al. (2021). Closed-loop neuromodulation in an individual with treatment-resistant depression. Nat. Med. *27*, 1696–1700.

9. Veloso, F., Kumar, K., and Toth, C. (1998). Headache secondary to deep brain implantation. Headache *38*, 507–515.

10. Raskin, N.H., Hosobuchi, Y., and Lamb, S. (1987). Headache may arise from perturbation of brain. Headache *27*, 416–420.

11. Lendvai, I.S., and Kinfe, T.M. (2017). Migraine Improvement After Anterior Thalamic Deep Brain Stimulation for Drug-Resistant Idiopathic Generalized Seizure: A Case Report. Headache *57*, 964–966.

12. Membrilla, J.A., Roa, J., and Díaz-de-Terán, J. (2023). Preventive treatment of refractory chronic cluster headache: systematic review and meta-analysis. J. Neurol. *270*, 689–710.

13. Fontaine, D., Lazorthes, Y., Mertens, P., Blond, S., Géraud, G., Fabre, N., Navez, M., Lucas, C., Dubois, F., Gonfrier, S., et al. (2010). Safety and efficacy of deep brain stimulation in refractory cluster headache: a randomized placebo-controlled double-blind trial followed by a 1-year open extension. J. Headache Pain *11*, 23–31.

14. Fontaine, D., Lanteri-Minet, M., Ouchchane, L., Lazorthes, Y., Mertens, P., Blond, S., Geraud, G., Fabre, N., Navez, M., Lucas, C., et al. (2010). Anatomical location of effective deep brain stimulation electrodes in chronic cluster headache. Brain *133*, 1214–1223.

15. Sheth, S.A., Bijanki, K.R., Metzger, B., Allawala, A., Pirtle, V., Adkinson, J.A., Myers, J., Mathura, R.K., Oswalt, D., Tsolaki, E., et al. (2022). Deep Brain Stimulation for Depression Informed by Intracranial Recordings. Biol. Psychiatry *92*, 246–251.

16. Li, Y., Chen, G., Lv, J., Hou, L., Dong, Z., Wang, R., Su, M., and Yu, S. (2022). Abnormalities in resting-state EEG microstates are a vulnerability marker of migraine. J. Headache Pain *23*, 45.

17. Zhang, N., Pan, Y., Chen, Q., Zhai, Q., Liu, N., Huang, Y., Sun, T., Lin, Y., He, L., Hou, Y., et al. (2023). Application of EEG in migraine. Front. Hum. Neurosci. *17*, 1082317.

18. Yuan, K., Zhao, L., Cheng, P., Yu, D., Zhao, L., Dong, T., Xing, L., Bi, Y., Yang, X., von Deneen, K.M., et al. (2013). Altered structure and resting-state functional connectivity of the basal ganglia in migraine patients without aura. J. Pain *14*, 836–844.

19. Schulte, L.H., Menz, M.M., Haaker, J., and May, A. (2020). The migraineur's brain networks: Continuous resting state fMRI over 30 days. Cephalalgia *40*, 1614–1621.

20. Xu, X., Zhou, M., Wu, X., Zhao, F., Luo, X., Li, K., Zeng, Q., He, J., Cheng, H., Guan, X., et al. (2023). Increased iron deposition in nucleus accumbens associated with disease progression and chronicity in migraine. BMC Med. *21*, 136.

21. Li, Z., Chen, Z., Fan, G., Li, A., Yuan, J., and Xu, T. (2018). Cell-Type-Specific Afferent Innervation of the Nucleus Accumbens Core and Shell. Front. Neuroanat. *12*, 84.

22. Salgado, S., and Kaplitt, M.G. (2015). The Nucleus Accumbens: A Comprehensive Review. Stereotact. Funct. Neurosurg. *93*, 75–93.

23. Massaly, N., Copits, B.A., Wilson-Poe, A.R., Hipólito, L., Markovic, T., Yoon, H.J., Liu, S., Walicki, M.C., Bhatti, D.L., Sirohi, S., et al. (2019). Pain-Induced Negative Affect Is Mediated via Recruitment of The Nucleus Accumbens Kappa Opioid System. Neuron *102*, 564–573.e6.

24. De Felice, M., Eyde, N., Dodick, D., Dussor, G.O., Ossipov, M.H., Fields, H.L., and Porreca, F. (2013). Capturing the aversive state of cephalic pain preclinically. Ann. Neurol. *74*, 257–265.

25. Amaral, V.C.G., Tukamoto, G., Kubo, T., Luiz, R.R., Gasparetto, E., and Vincent, M.B. (2018). Migraine improvement correlates with posterior cingulate cortical thickness reduction. Arq. Neuropsiquiatr. *76*, 150–157.

26. Peek, A.L., Leaver, A.M., Foster, S., Puts, N.A., Oeltzschner, G., Henderson, L., Galloway, G., Ng, K., Refshauge, K., and Rebbeck, T. (2021). Increase in ACC GABA+ levels correlate with decrease in migraine frequency, intensity and disability over time. J. Headache Pain *22*, 150.

27. Peek, A.L., Leaver, A.M., Foster, S., Oeltzschner, G., Puts, N.A., Galloway, G., Sterling, M., Ng, K., Refshauge, K., Aguila, M.E.R., and Rebbeck, T. (2021). Increased GABA+ in People With Migraine, Headache, and Pain Conditions- A Potential Marker of Pain. J. Pain *22*, 1631–1645.

28. Russo, A., Tessitore, A., Esposito, F., Di Nardo, F., Silvestro, M., Trojsi, F., De Micco, R., Marcuccio, L., Schoenen, J., and Tedeschi, G. (2017). Functional Changes of the Perigenual Part of the Anterior Cingulate Cortex after External Trigeminal Neurostimulation in Migraine Patients. Front. Neurol. *8*, 282.

29. Smith, M.L., Asada, N., and Malenka, R.C. (2021). Anterior cingulate inputs to nucleus accumbens control the social transfer of pain and analgesia. Science *371*, 153–159.

30. Gao, S.H., Shen, L.L., Wen, H.Z., Zhao, Y.D., Chen, P.H., and Ruan, H.Z. (2020). The projections from the anterior cingulate cortex to the nucleus accumbens and ventral tegmental area contribute to neuropathic pain-evoked aversion in rats. Neurobiol. Dis. *140*, 104862.

31. Hamani, C., Schwalb, J.M., Rezai, A.R., Dostrovsky, J.O., Davis, K.D., and Lozano, A.M. (2006). Deep brain stimulation for chronic neuropathic pain: long-term outcome and the incidence of insertional effect. Pain *125*, 188–196.

32. Hamani, C., Fonoff, E.T., Parravano, D.C., Silva, V.A., Galhardoni, R., Monaco, B.A., Navarro, J., Yeng, L.T., Teixeira, M.J., and de Andrade, D.C. (2021). Motor cortex stimulation for chronic neuropathic pain: results of a double-blind randomized study. Brain *144*, 2994–3004.

33. Tykocki, T., Nauman, P., Koziara, H., and Mandat, T. (2013). Microlesion effect as a predictor of the effectiveness of subthalamic deep brain stimulation for Parkinson's disease. Stereotact. Funct. Neurosurg. *91*, 12–17.

34. Krusz, J.C., Scott, V., and Belanger, J. (2000). Intravenous propofol: unique effectiveness in treating intractable migraine. Headache *40*, 224–230.

35. Vosoughian, M., Saeedi, N., Moshari, M., Dabir, S., Dahi, M., Tabashi, S., Haji Naghi Tehrani, K., and Hajizadeh, N. (2021). The Effect of Propofol Anesthesia on the Pain Severity and Frequency of Migraine Attacks in Patients with Chronic Migraine Headache over a Six Month Follow Up: An Observational Study. Iran. J. Pharm. Res. *20*, 415–421.

36. Mestre, T.A., Lang, A.E., and Okun, M.S. (2016). Factors influencing the outcome of deep brain stimulation: Placebo, nocebo, lessebo, and lesion effects. Mov. Disord. *31*, 290–296.

37. Keitel, A., Wojtecki, L., Hirschmann, J., Hartmann, C.J., Ferrea, S., Südmeyer, M., and Schnitzler, A. (2013). Motor and cognitive placebo-/nocebo-responses in Parkinson's disease patients with deep brain stimulation. Behav. Brain Res. *250*, 199–205.

38. Kaptchuk, T.J., Goldman, P., Stone, D.A., and Stason, W.B. (2000). Do medical devices have enhanced placebo effects? J. Clin. Epidemiol. *53*, 786–792.

39. Sacco, S., Braschinsky, M., Ducros, A., Lampl, C., Little, P., van den Brink, A.M., Pozo-Rosich, P., Reuter, U., de la Torre, E.R., Sanchez Del Rio, M., et al. (2020). European headache federation consensus on the definition of resistant and refractory migraine : Developed with the endorsement of the European Migraine & Headache Alliance (EMHA). J. Headache Pain *21*, 76.

40. Brennan, K.C., and Pietrobon, D. (2018). A Systems Neuroscience Approach to Migraine. Neuron *97*, 1004–1021.

41. Skorobogatykh, K., van Hoogstraten, W.S., Degan, D., Prischepa, A., Savitskaya, A., Ileen, B.M., Bentivegna, E., Skiba, I., D'Acunto, L., Ferri, L., et al. (2019). Functional connectivity studies in migraine: what have we learned? J. Headache Pain *20*, 108.

42. Chen, Y.-W., and Lin, C.-J. (2006). Combining SVMs with Various Feature Selection Strategies. In Feature Extraction: Foundations and Applications, I. Guyon, M. Nikravesh, S. Gunn, and L.A. Zadeh, eds. (Springer Berlin Heidelberg), pp. 315–324.

STAR★METHODS

KEY RESOURCES TABLE

REAGENT or RESOURCE	SOURCE	IDENTIFIER
Software and algorithms		
MATLAB	MathWorks, R2021b, U.S.	https://ww2.mathworks.cn/

RESOURCE AVAILABILITY

Lead contact

(1) Further information and requests for resources and reagents should be directed to and will be fulfilled by the lead contact, Zhao Dong (dong_zhaozhao@126.com).

Materials availability

This study did not generate new unique reagents.

Data and code availability

(1) All data produced in this study are included in the published article and its supplemental information, or are available from the lead contact upon request.
(2) This paper does not report original code.
(3) Any additional information required to reanalyze the data reported in this paper is available from the lead contact upon request.

EXPERIMENTAL MODEL AND STUDY PARTICIPANT DETAILS

Participant

The patient was a young man who had been experiencing bilateral temporal throbbing headaches for over 5 years. These migraine attacks were accompanied by a Visual Analogue Scale (VAS) score ranging from 2 to 6, with a frequency of two to three times per week and duration lasting from 4 to 12 h. Additionally, the attacks were often accompanied by symptoms such as nausea, vomiting, photophobia, phonophobia, and various autonomic symptoms (e.g., moist eyes, tearing, and yawning), significantly disrupting the patient's daily activities. Over time, the number of attacks gradually increased, eventually leading to a constant headache with a VAS score of 3–4 and multiple exacerbations throughout the day. The exacerbations were triggered by factors such as consuming cola or coffee, as well as hunger. The psychology department simultaneously assisted in excluding the possibility of anxiety or depression. Based on the third edition of the International Classification of Headache Disorders (ICHD-3), the patient was diagnosed with chronic migraine. Despite multiple hospitalizations and various treatments, including antidepressants, antiepileptics, beta-blockers, calcium channel blockers, and onabotulinumtoxin A, as well as non-pharmacological interventions, only slight improvement in symptoms was observed. With a lack of responsiveness to these treatments, the patient's case was deemed consistent with refractory migraine.[39] Following a comprehensive evaluation and careful observation, the patient underwent SEEG in preparation for precise DBS.

Standard protocol approvals, registrations, and patient consents

The study was approved by the Ethics Committee of the Chinese PLA General Hospital. The patient provided written informed consent to participate in this research. The study was carried out in accordance with the World Medical Association's Declaration of Helsinki.

METHOD DETAILS

Surgical procedure

The patient underwent the SEEG electrode implantation procedure as follows. According to previous research, we implanted 14 SEEG electrodes (Beijing Sinovation Medical Technology Co., Ltd., Beijing, China) in the bilateral periaqueductal/periventricular gray area (PAG/PVG), ventral posteromedial and posterolateral (VPM/VPL), NAc, dACC, posterior hypothalamus, amygdala (AMY), and insula (IS), which have shown the most promise for symptomatic improvement[40,41] (Figure 1A). The electrodes utilized in this study were characterized by a diameter of 0.8 mm, consisting of 10–20 contacts. Each contact possessed an electrode point length of 2 mm and an electrode point spacing of 1.5 mm. The surgical plan was created with Reme-Studio, and the procedure was carried out with the assistance of a Remebot neurosurgical robot (Beijing Baihui Weikang Technology Co., Ltd., Beijing, China). The electrode positions were confirmed intraoperatively using computed tomography. No complications occurred during the procedure. The electrodes were completely removed after 12 days of clinical monitoring and intracranial stimulation.

Clinical measures of migraine and associated comorbidities

We used the VAS score to evaluate moment-to-moment changes in attack severity. The patient was instructed to maintain a written diary at regular intervals in order to minimize external interruptions. The recorded data were reported on a daily basis to a member of the research team for prompt communication. The 14-month preoperative headache diary recording and training of the recording paradigm in the patient's first 2 days postoperatively ensured accuracy of the measurement of clinical symptoms. Microsoft Excel was used to collect and manage the study data. The patient underwent the entire procedure in our ward, remaining as calm and bedridden as possible to reduce disruption during the recording. During the clinical monitoring phase, considering that no further headache attacks had occurred, we induced migraine with the patient's typical previous triggers. He recorded his VAS scores for 7 days in 5-min increments and electrophysiological data in real time (Figure 1B). According to the distribution of the VAS dataset, we eliminated the mid-range values and categorized the dataset into 'high' and 'low' symptoms to ensure the robustness of the results (Figure 2A). Furthermore, the aforementioned associated symptoms were recorded during headache attacks.

Clinical-electrophysiological mapping via electrode stimulation

We tested the clinical effect of a set of stimulation parameters (10, 50, or 100 Hz; 300 μs; 1–5 mA) through a systematic bipolar stimulation survey and blinded sham-controlled stimulation studies. To start, a 30-s stimulus duration was employed to test for potential adverse effects and to initially evaluate the set of stimulus parameters that resulted in alterations in headache severity, followed by a 90-s stimulus setting for candidate targets. To minimize the potential for bleed over effects from one stimulation site to another, a 60-s washout period was included between stimuli to minimize the potential for bleed over effects from one stimulation site to another. The brain stimulation configuration was depicted by contact number and polarity (for example, 2-/3+ indicates that contact 2 is a cathode and contact 3 is an anode). The stimulus procedure consists of four rounds in total, divided into two steps. First, we performed mapping of different parameters in all brain regions of interest to determine preliminarily the corresponding headache severity and other responses (Figure 1C). The process was repeated twice and performed blinding to the stimulation order, stimulation time, and other parameters. The candidate brain regions were chosen based on their ability to provide relief from headaches without eliciting severe discomfort responses. Secondly, we thoroughly screened and validated the ultimate targets for stimulation from multiple perspectives, encompassing diverse stimulation durations and alternating between true and sham stimuli. The blinding approach encompassed participants, study personnel, and outcome assessors. Participants were blinded to stimulus parameters, stimulus onset and end times. Study personnel were blinded to the assessment of the results. Additionally, an extra member of the study personnel was designated for outcome assessment and remained blinded to the stimulation procedure as well as trial records.

Signal processing

Real SEEG recordings were collected from the 14 SEEG electrodes with a sampling rate of 1000 Hz. All recordings were preprocessed with a 50-Hz comb notch filter to remove the line noise frequency and its harmonics, followed by a 0.5- to 300-Hz bandpass filter to eliminate baseline shifting; they were then re-referenced to the common average across all channels.[8] To identify spectral biomarkers related to symptom severity states, 5-min epochs after each self-reported VAS score were segmented for further spectral analyses. The spectral power for each channel was calculated at 30-s intervals and averaged over a 5-min recording period using the Morlet wavelet transform (center frequency = 6 Hz). The seven frequency bands of interest were delta (δ, 1–4 Hz), theta (θ, 4–8 Hz), alpha (α, 8–12 Hz), beta (β, 12–30 Hz), low gamma (Lγ, 30–70 Hz), high gamma (Hγ, 70–150 Hz, and high-frequency oscillation (HFO) (150–300 Hz), yielding seven power features for each channel included (7 bands × 56 channels). Finally, the power feature for each brain region was determined by the spectral power averaged across all contacts within the brain regions (7 bands × 14 regions). All analyses were conducted using MATLAB R2021b (MathWorks, Natick, MA).

Biomarker discovery for headache states representation

We determined the spectral power features of specific brain regions that were predictive of symptom severity using statistical analyses and cross-validated machine-learning models (Figure 1D). First, to investigate the relationship between the derived spectral power features and VAS score, Spearman's correlation coefficient (rho) along with its p value were calculated for all features and montages. Furthermore, the two-sided Wilcoxon rank-sum test was used to validate whether a derived feature could significantly distinguish between low and high-symptom severity, yielding a p value for each feature, which was considered significant at the $\alpha = 0.05$ level. Next, to minimize the high dimensionality of features and enhance the overall performance of the machine-learning classifier, the F-score feature selection method was implemented.[42] The weight for a given feature was calculated using the F-score method. Greater weights contributed more to the migraine severity classification. Features with weights greater than 0.25 and p values less than 0.05 were fed into different machine-learning classifiers, including decision trees (DT), linear discriminant analysis (LDA), logistic regression (LR), Naive Bayes (NB), and support vector machines (SVM). Their performances were assessed using the accuracy, sensitivity, specificity, F1-score, and area under the receiver operating characteristic (ROC) curve (AUC).

QUANTIFICATION AND STATISTICAL ANALYSIS

Microsoft Excel was used to collect and manage the study data. Real SEEG recordings were collected from the 14 SEEG electrodes with a sampling rate of 1000 Hz. All recordings were preprocessed with a 50-Hz comb notch filter to remove the line noise frequency and its harmonics, followed by a 0.5- to 300-Hz bandpass filter to eliminate baseline shifting; they were then re-referenced to the common average across all channels.[8] To identify spectral biomarkers related to symptom severity states, 5-minute epochs after each self-reported VAS score were segmented for further spectral analyses. The spectral power for each channel was calculated at 30-second intervals and averaged over a 5-minute recording period using the Morlet wavelet transform (center frequency = 6 Hz). The seven frequency bands of interest were delta (δ, 1–4 Hz), theta (θ, 4–8 Hz), alpha (α, 8–12 Hz), beta (β, 12–30 Hz), low gamma (Lγ, 30–70 Hz), high gamma (Hγ, 70–150 Hz, and high-frequency oscillation (HFO) (150–300 Hz), yielding seven power features for each channel included (7 bands × 56 channels). Finally, the power feature for each brain region was determined by the spectral power averaged across all contacts within the brain regions (7 bands × 14 regions). All analyses were conducted using MATLAB R2021b (MathWorks, Natick, MA).